Helicopter load alleviation using active control

M. Voskuijl, D. J. Walker and B. J. Manimala
Department of Engineering
The University of Liverpool
Liverpool, UK

ABSTRACT

This paper discusses how structural load objectives can be included in a rotorcraft flight control system design in an efficient and straightforward way using multivariable control techniques. Several research studies have indicated that pitch link loads for various rotorcraft types can reach high or even unacceptable values, both in steady state and maneuvering flight. This is especially the case for high-speed aggressive maneouvers. Pitch link loads at high-speed flight are therefore taken as a case study. A novel longitudinal control system is presented, designed to reduce helicopter pitch-link loads during high-speed longitudinal manoeuvres whilst providing a pitch attitude command attitude hold response type. The design is based on a high-order model of a helicopter representative of the UH-60 Black Hawk. New metrics are presented for the analysis of structural loads that can be used in combination with ADS-33 handling qualities requirements.

NOMENCLATURE

D	damage [-]
F	load [lbf]
g	gravitational acceleration [m/s^2]
K	controller matrices
M_x	pitching moment at the blade root [lbf-ft]
$M_{x,Coleman}$	Coleman transformation of the pitch link load [ft-lbf]
N	number of cycles [-]
N_i	number of cycles at failure [-]
$n_{z,qs}^{pk}$	peak quasi-steady normal acceleration defined w.r.t. level flight (g's)
$n_{z,pk}^{vib}$	the peak amplitude in the vibratory components of the hub forces [g's]
P	plant matrices
q	pitch rate [rad/s]
Q_γ	agility quickness [1/sec]
Q_θ	attitude quickness [1/sec]
Q_l	load quickness [lbf/deg]
r	yaw rate [rad/s]
S	stress [lbf / ft^2]
t	time [s]
$\mathbf{u}$	vector of control variables
$\mathbf{v}$	vector of measured variables
$\mathbf{w}$	vector of exogenous variables (reference, disturbance)
$\mathbf{z}$	vector of 'error' signals

Greek notation

α	angle-of-attack [rad]
β_{1c}	longitudinal flapping angle [rad]
γ	flight path angle [rad]
Δ	change
θ	pitch attitude [rad]
θ_0	collective pitch angle [rad] (positive – climb)
θ_0,τ_r	tail rotor collective pitch angle [rad] (positive – left yaw)
θ_{1c}	lateral cyclic pitch [rad] (positive – right roll)
θ_{1s}	longitudinal cyclic pitch [rad] (positive – nose down)
ω	frequency [rad/s]
Ω	rotor rotational speed [rad/s]
ψ	azimuth angle [rad]

Paper No. 3181. Manuscript received 6 February 2007, revised 8 May 2008, second revision 25 June 2008, accepted 4 August 2008.

https://doi.org/10.1017/S0001924000002633 Published online by Cambridge University Press

Subscripts

a	amplitude
max	maximum
min	minimum
MTE	mission task element
pk	peak
pl	pitch link
ref	reference
sla	structural load alleviation
ss	steady state
12	between borders 1 and 2
23	between borders 2 and 3
34	between borders 3 and 4

Abbreviations

ACAH	attitude command attitude hold
CFH	carefree handling
FAR	Federal Aviation Regulations
JAR	Joint Aviation Requirements
FEP	flight envelope protection
FGR	Flightlab Generic Rotorcraft
HELI-ACT	helicopter active control technology
HQ	handling qualities
IAS	indicated airspeed
LAF	load amplification factor
MBC	multi blade co-ordinates
MTE	mission task element
NACA	National Advisory Committee for Aeronautics
RC	rate command
SCAS	stability command augmentation system
SLA	structural load alleviation
UTTAS	Utility Tactical Transport Aerial System

1.0 INTRODUCTION

Helicopters and other rotorcraft such as tilt-rotors have relatively poor stability and control characteristics compared to conventional fixed-wing aircraft. These characteristics, which are generally worse in the low-speed flight regime, are inherent to the rotor system that provides the vertical lift capability. Other difficulties can occur when a rotorcraft is operated close to the limits of its flight envelope. Structural loads can then reach high to unacceptable values and limits have to be monitored, which poses an extra workload on the pilot. The development of computers, fly-by-wire flight control systems and lightweight accurate sensors has made it possible for the flight control engineer to design elaborate automatic flight control systems (AFCS)[1] that can provide a wide range of functions, from basic stabilisation to advanced envelope protection schemes and autopilots. Active control technology could potentially make it possible to utilise the maximum performance capabilities of a given rotorcraft in a safe manner without exceeding any structural limits and preferably with a low pilot workload. The ability to fly throughout the operational flight envelope without concern for structural, aerodynamic or control limits is referred to as 'carefree handling' (CFH)[2].

The research presented in this paper is part of the helicopter active control technology (HELI-ACT) project[3,4], which involves collaboration between the University of Liverpool and the National Research Council (NRC) of Canada. The project, which lasted from 2003 until 2007, has had access to a six-axis motion base flight simulator HELI-FLIGHT[5] at the University of Liverpool and a fly-by-wire research Bell 412 helicopter at the NRC[6,7]. Furthermore, high fidelity nonlinear helicopter and tilt rotor simulation models were available as test subjects. The broad aim of the project is to develop new control concepts for:

1. Handling qualities (HQ) improvement
2. Structural load alleviation (SLA)
3. Flight envelope protection (FEP)

An AFCS should have all the required sub-functions derived from these three main objectives integrated in one system. This paper discusses how structural load objectives can be included in the flight control system design in an efficient and straightforward way using multivariable control techniques. A novel control system is presented, designed to reduce helicopter pitch-link loads during high-speed pull up manoeuvres. The design is based on a high-order model of a helicopter representative of the UH-60 Black Hawk. The paper presents an analysis of the control law. There are no generally accepted or established metrics for the evaluation of structural loads that can be used in conjunction with ADS-33 handling qualities requirements for the evaluation of mission task elements (MTE). The second aim of this paper is therefore the definition of new load metrics.

Several research studies[8-12] have indicated that pitch link loads for various rotorcraft types can reach high or unacceptable values, both in steady state and manoeuvring flight. This is especially the case for high-speed aggressive manoeuvres. Protecting the pitch links from high transient loads is potentially the type of functionality that might be desirable in a future CFH system. The Flightlab Generic Rotorcraft (FGR) simulation model is used in this paper as the primary research tool. The FGR is similar to the UH-60A Black Hawk helicopter. This model has a selective level of fidelity. The main modeling features of the FGR selected for the purpose of this paper are the following. The rotor system is modeled as a rigid blade element model with a three-state inflow model and quasi-steady air loads. Aerodynamic data of the blades is stored in look-up tables as a function of the angle of attack, Mach number and Reynolds number. The aerodynamics of the fuselage, vertical tail and horizontal tail are also stored in look-up tables. The fuselage structure is modeled as rigid. A detailed dynamic model of the turboshaft engines and drive train is present as well. The tail rotor is modeled as a Bailey rotor[13]. Finally, the stability command augmentation system (SCAS) is removed from the model because this allows the implementation of novel control laws and the evaluation of the bare airframe dynamic behavior. Clearly, the design of an active control system for pitch link loads requires a good understanding of the nature of the loads acting on the pitch link. Flight tests and/or simulations can be performed to analyse the behaviour of the pitch link loads at various flight conditions. The correct prediction of pitch link loads is a difficult task and the level of modelling used in this paper is merely good enough to predict the general trend. However, this is not an issue since it is not the intention of this paper to accurately represent the pitch link loads. The main aim of the research is to develop a design method for structural load alleviation control laws. This method should be applicable to a variety of structural loads, including loads in the rotating frame. The pitch link loads of the FGR are taken as a test-case.

Accurate modelling of helicopter flight dynamics is in general quite difficult due to the interaction of many complex physical phenomena such as the rotor wake. For example, the correct prediction of the off-axis response remains an issue in many helicopter models[14]. Accurate modelling becomes even more difficult when certain data such as blade elastic properties are not available. Even more difficult to model are helicopter vibratory loads. Helicopter models are therefore subject to modelling uncertainties. Here, model uncertainty is defined as the difference between the actual system and the model of the system. It is therefore eminent that structural load alleviation control laws for helicopters should be designed with a robust control method that is particularly useful for control of uncertain systems.

The structure of this paper is as follows. The next section will describe the analysis of the pitch link loads for the FGR simulation model. The manoeuvre of interest is a high-speed pull-up

https://doi.org/10.1017/S0001924000002633 Published online by Cambridge University Press

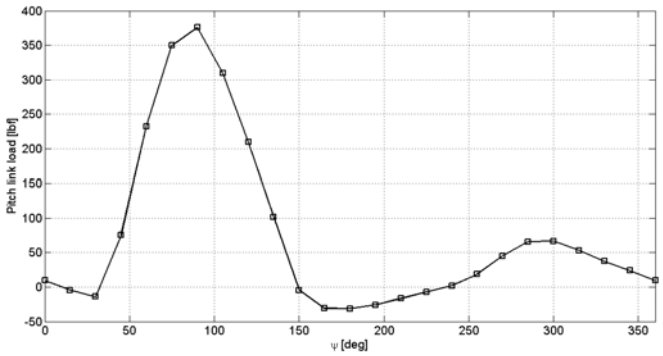


Figure 1. Pitch link load as a function of rotor azimuth in steady level flight at 120kt.

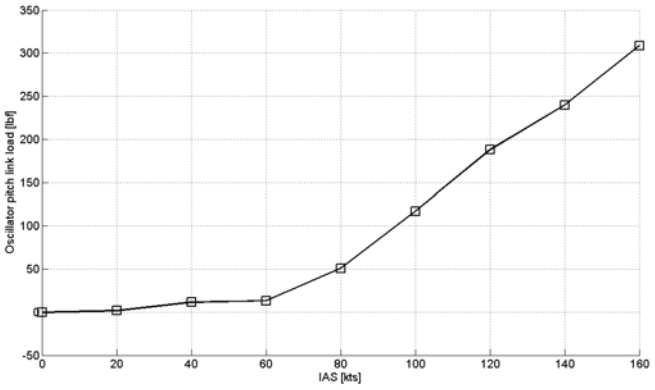


Figure 2. Oscillatory pitch link load as a function of flight speed.

manoeuvre. Section 3 introduces the newly proposed design method for a flight control laws that include structural load alleviation objectives. This method is then applied in Section 4 to the design in the linear domain of a longitudinal flight control law that provides a pitch attitude command attitude hold response type combined with a pitch link load alleviation objective. This controller is subsequently analysed on the non-linear FGR simulation model and tested in a series of desktop simulations. New load metrics are presented for the analysis. Finally conclusions and recommendations are drawn.

2.0 LOADS ANALYSIS

The pitch link loads of the FGR are investigated through desktop simulations in this section. The first section treats the pitch link loads in steady state trimmed forward flight. This is followed by a paragraph in which the transient pitch link loads are evaluated during a simulated 2g pull up manoeuvre at 120kt forward flight. Two high-speed pull-up manoeuvres from level flight were performed during flight tests of the NASA/Army UH-60A air loads programme[9,15]. These pull-ups were designated as the UTTAS (Utility Tactical Transport Aerial System) manoeuvre. This manoeuvre is specified as a pull-up from level flight during which a load factor of 1·75g was held without losing more than 30kt of airspeed. One UTTAS manoeuvre was executed at 150kt IAS and a load factor of 1·8g. The second UTTAS manoeuvre was performed from 130kt IAS and a load factor of 2·1g. The UH-60A used in the air loads program was highly instrumented for the flight test and results indicated that pitch link loads increased significantly during the manoeuvre.

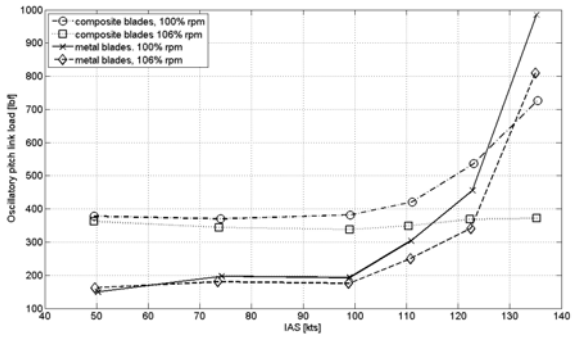


Figure 3. S-61 oscillatory pitch link load as a function of flight speed[8].

2.1 Pitch link loads in forward flight

Figure 1 shows the variation of the FGR pitch link load as a function of rotor azimuth at a simulated flight condition of 120kt straight-and-level. This flight condition is the start point for the pull-up manoeuvre described in the next section. The pitch link load is small over a large portion of the rotor disk and increases on the advancing blade side, where a large peak occurs (Note that positive loads are tensile). Figure 2 shows the magnitude of the oscillatory pitch link load as a function of flight speed. This is defined as half of the peak-to-peak variation over one azimuth. The oscillatory pitch link load is low for flight speeds up to 60kt and then starts to increase in fairly a linear manner.

The typical trend for steady-state pitch link loads on a newly designed helicopter in its first flight test is that they increase significantly with increasing flight speed. They will even exceed the endurance limit above certain airspeed in some cases[1]. Important to note is that this general trend for pitch link loads is present in the FGR simulation model; i.e. increasing loads with flight speed.

Flight test data of a different helicopter type, the Sikorsky S-61 helicopter[8], are presented in Fig. 3 as an illustration. Two blade designs are compared at two rotor speeds. This figure illustrates that oscillatory pitch link loads can increase significantly as a function of airspeed. Research on the S-61[8,16] has indicated that the use of advanced airfoils and an improved blade design have produced a significant reduction in the pitch link loads.

2.2 Pitch link loads in high-speed pull up manoeuvres

The transient pitch link loads during a 2g pull-up manoeuvre from level flight are investigated in this paragraph. This manoeuvre is very similar to the UTTAS manoeuvre as described in the introduction of this section. The structural envelope of the UH-60A[9] allows manoeuvres up to 3·5g at this speed. So this manoeuvre is executed well within the structural flight envelope of the FGR. The pull-up is executed with a simple longitudinal stick step input after 1 second steady flight. The amplitude of the stick input is chosen such that the load factor in the manoeuvre equals 2g. In this case 15% of full-scale stick deflection is required to encounter 2gs. The lateral/directional states of the model are kept close to their trim values by a classical flight control law in these channels; it provides an ACAH in roll and a RC response type in yaw. This control law was designed solely for the purpose of assisting this manoeuvre. The load factor encountered due to such an input is close to 2g. The flight speed at the start of the manoeuvre is 120kt. The resulting transient pitch link load on one blade is presented in Fig. 4.

There is a large increase in the oscillatory pitch link load during the pull-up and it goes from tensile to compressive. Parts of the rotor

https://doi.org/10.1017/S0001924000002633 Published online by Cambridge University Press

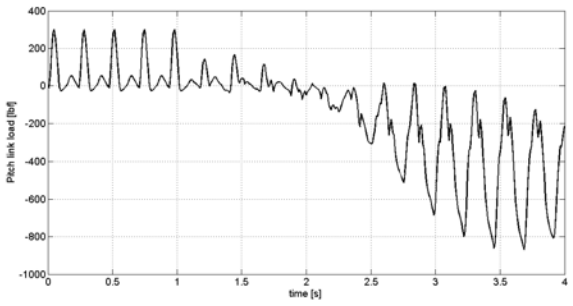


Figure 4. Transient pitch link loads for a 2g pull-up manoeuvre at 120kt.

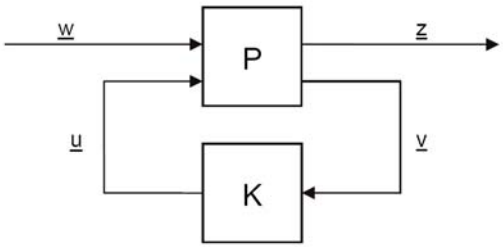


Figure 5. General control configuration.

disk on the retreating blade side are in deep stall during the 2g pull, which results in pitching down moments on the rotor blades and thus a compressive stress on the pitch link. The increase is approximately 160% of the steady state value. Thus the general trend of increasing pitch link loads for the UTTAS manoeuvre in the UH-60A airloads program is also observed on the FGR simulation model. Thus it is reasonable to use the FGR in a case study focussed on new design methods for structural load alleviation flight control laws.

3.0 DESIGN METHOD FOR STRUCTURAL LOAD ALLEVIATION

The proposed load alleviation design method is based on H-infinity optimisation. Figure 5 shows the generalised control configuration, consisting of the generalised plant (*P*) and the feedback controller (*K*); **w** is the vector of reference signals, **z** is the vector of error signals, **v** is the vector of feedback variables and **u** is the vector of control variables. *H*-infinity optimisation is used to obtain a stabilising controller transfer function that minimises the energy gain from the vector of reference signals to the vector of error signals. The rationale for using the H-infinity control method is twofold. First, the proposed method enables handling qualities objectives, such as providing a pitch ACAH response type, to be combined with structural load objectives, such as reducing the pitch link load. This is accomplished by including appropriate signals in the vector **z**. Second, *H*-infinity control is particularly useful for control of uncertain systems. As explained in the introduction, the FGR structural loads are subject to model uncertainties. In 2005, the first successful flight test of an *H*-infinity control law on a Bell 412 helicopter was demonstrated in the HELI-ACT project in 2005[17]. This control law was based on a rotorcraft model[3] with uncertainties present. This demonstrates that *H*-infinity control is a useful technique applicable to a real helicopter. An introduction into *H*-infinity control can be found in Ref. 18.

The design method consists of the following steps.

- Linearise the non-linear model, with output equations that include the structural load envelope
- Analyse the problem and determine which controls and feedback variables are available
- Set goals with respect to handling qualities and structural load alleviation
- Set up a general control configuration and include the goals from the previous step in the vector of error signals '**z**'
- Synthesise an *H*-infinity controller for the general control configuration that fulfils handling qualities and structural load objectives simultaneously
- Implement the controller on the nonlinear simulation model and analyse

This is an iterative design process that can take several iterations before the final control law that fulfils all requirements is achieved. Note that the structural load of interest does not necessarily have to be amongst the feedback variables into the controller. The process is applied to the case study of pitch link loads in high-speed pull-ups for the FGR in the next section.

4.0 CONTROL LAW DESIGN

The main goal of the case study is to design two flight control laws for one specific high-speed flight condition. Both controllers should make it possible to perform aggressive pull-up manoeuvres. One controller however should provide structural load alleviation for the pitch link loads. A trade-off therefore has to be made between handling qualities and structural loads. The purpose of the control laws is to demonstrate the method of designing a structural load alleviation control law as presented in the previous section. In principle, the design process presented can be applied to design a fully optimised flight control law for the complete high speed flight regime. It is not the intention to design a fully optimised flight control law but first, to demonstrate the effectiveness if the design process and second, to introduce new structural load metrics for the analysis of the flight control laws. Typically speaking, a longitudinal flight control law for a helicopter will provide the pilot with a pitch RC, a pitch ACAH or a load factor demand response type. It is decided in this case to provide a pitch ACAH response type. The rationale for choosing an ACAH response type is to provide a sufficient level of stability in degraded visual conditions. The control law design and analysis presented in the next sections could also be done when a RC or load factor response type was chosen. The design method outlined in Section 3 is used for the control law design in the next paragraph. The first control law is designated by 'SLA' and the second controller is designated by 'conventional'.

4.1 Longitudinal multi-objective flight control law design

A linear model of the FGR is required for control law design. However, the oscillatory pitch link loads cannot be linearised in the usual manner because they are variables in the individual blade co-ordinates. A Coleman transformation is therefore used to represent the loads acting on the individual blades in multi-blade co-ordinates (MBC)[19-21].

$$\begin{bmatrix} M_{x0} \\ M_{xc} \\ M_{xs} \end{bmatrix} = \frac{1}{4} \begin{bmatrix} 1 & 1 & 1 & 1 \\ 2\mathrm{C}\cos\psi_1 & 2\mathrm{C}\cos\psi_2 & 2\mathrm{C}\cos\psi_3 & 2\mathrm{C}\cos\psi_4 \\ 2\mathrm{S}\sin\psi_1 & 2\mathrm{S}\sin\psi_2 & 2\mathrm{S}\sin\psi_3 & 2\mathrm{S}\sin\psi_4 \end{bmatrix} \begin{bmatrix} M_{x1} \\ M_{x2} \\ M_{x3} \\ M_{x4} \end{bmatrix}$$

$$M_{x,Coleman} = M_{x0} + M_{xc} + M_{xs} \quad \ldots (1)$$

https://doi.org/10.1017/S0001924000002633 Published online by Cambridge University Press

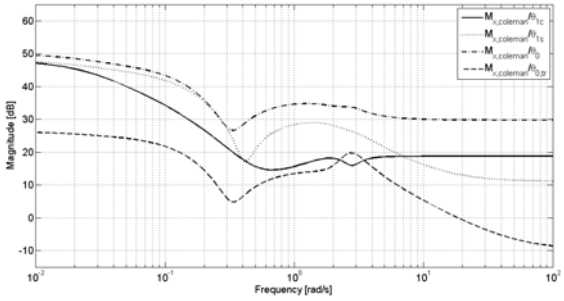


Figure 6. Open loop frequency response of pitch link load envelope ($M_{x,Coleman}$).

The load envelope $M_{x,Coleman}$ represents the dominant effect of the pitch link loads acting on the four blades when performing a manoeuvre. This transformation is foreseen to be accurate enough for control law design as will be shown in this section. A nine-state linear model of the FGR at 120kt in trimmed level forward flight, with a pitch link load envelope ($M_{x,Coleman}$) as one of the outputs, is obtained from the non-linear FGR simulation model. An open loop frequency response is performed to evaluate the influence of the different control inputs on the pitch link load envelope (Fig. 6).

The open loop frequency response shows that both collective pitch angle and longitudinal cyclic pitch have the largest effect of all the control inputs on the pitch link load envelope. These are also the main controls that are used for controlling the longitudinal states of the aircraft in high-speed flight. It therefore makes sense to design a multivariable longitudinal controller that has these two controls as outputs. The selected feedback signals for the controller are the pitch attitude and rate. These are chosen because they are typically available for feedback on a production aircraft. The controller is synthesised using H_∞ optimisation and the complete feedback control system is shown in Fig. 7.

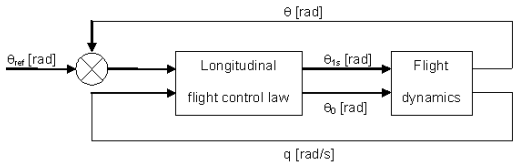


Figure 7. Longitudinal high-speed flight control law.

The controller matrices are derived with the MATLAB® algorithm hinflmi[22]. The signals needed for the general control configuration are the following.

$$\mathbf{z}_{\mathbf{sla}} = \begin{bmatrix} \theta_{ref} - \theta & M_{x,Coleman} & \theta_{1s} & \theta_0 \end{bmatrix}$$
$$\mathbf{v}_{\mathbf{sla}} = \begin{bmatrix} \theta & q \end{bmatrix}$$
$$\mathbf{w}_{\mathbf{sla}} = \begin{bmatrix} \theta_{ref} \end{bmatrix}$$
$$\mathbf{u}_{\mathbf{sla}} = \begin{bmatrix} \theta_{1s} & \theta_0 \end{bmatrix}$$

$$\mathbf{z}_{\mathbf{conventional}} = \begin{bmatrix} \theta_{ref} - \theta & \theta_{1s} & \theta_0 \end{bmatrix}$$
$$\mathbf{v}_{\mathbf{conventional}} = \begin{bmatrix} \theta & q \end{bmatrix}$$
$$\mathbf{w}_{\mathbf{conventional}} = \begin{bmatrix} \theta_{ref} \end{bmatrix}$$
$$\mathbf{u}_{\mathbf{conventional}} = \begin{bmatrix} \theta_{1s} & \theta_0 \end{bmatrix}$$

H_∞ optimisation was used to synthesise a stabilising controller transfer function K that minimised the energy-gain from w to z. Frequency dependent weights and simple gains were set on the vector of error signals to obtain a pitch ACAH response type and, in the case with SLA, an acceptable load reduction. The resulting controllers were implemented on the nonlinear FGR simulation model and a pull-up following a step input in longitudinal stick was investigated (Figs 8-10).

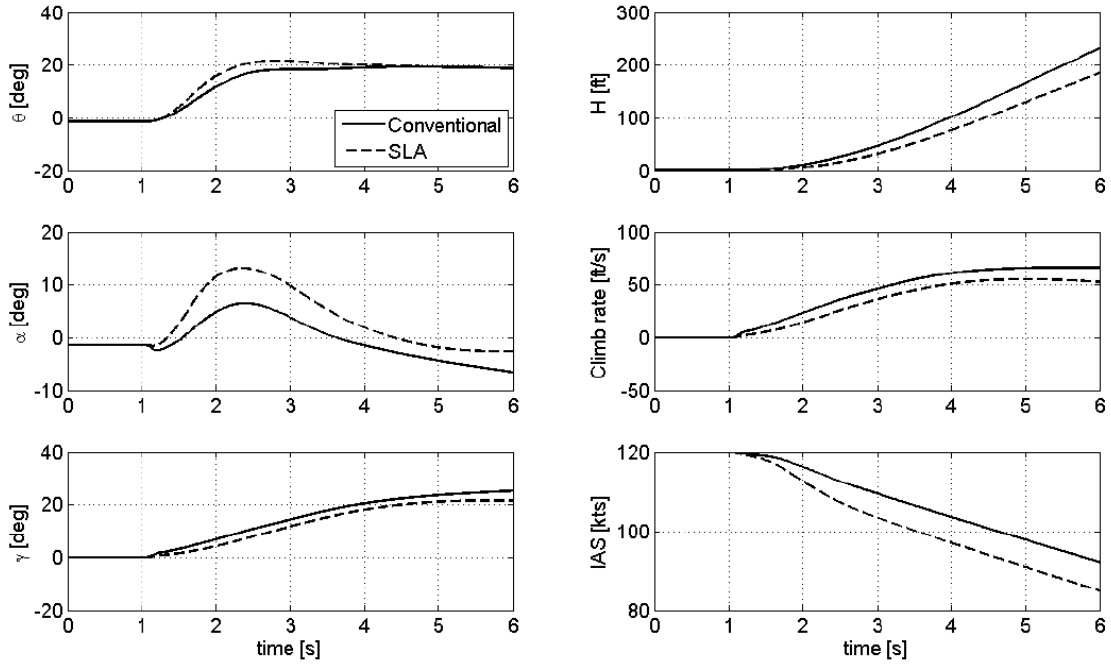


Figure 8. Evaluation of aircraft response for conventional and SLA controller.

https://doi.org/10.1017/S0001924000002633 Published online by Cambridge University Press

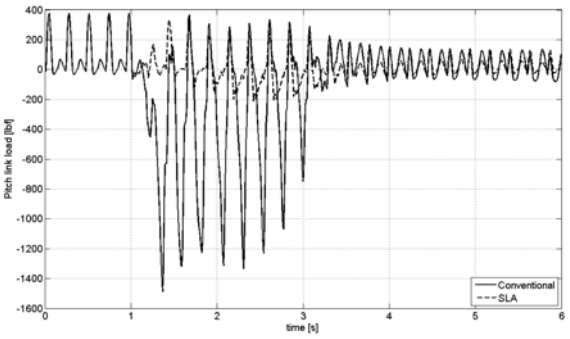


Figure 9. Evaluation of pitch link loads for two control laws on the FGR.

First, the performance in terms of handling qualities is discussed briefly. The response in terms of pitch attitude is similar for both control laws. A measure for comparing the moderate amplitude agility is the ADS-33 pitch attitude quickness parameter (Equation 2).

$$Q_\theta = \frac{q_{pk}}{\Delta\theta_{pk}} \quad \ldots (2)$$

The pitch attitude quickness for the conventional control law is 0·97 compared to 1·17 for the SLA control law. However, the achieved flight path angle in the pull-up is smaller. This can also be seen when the altitude and climb rate are evaluated. In Section 4.3 it will be shown that the maximum achievable flight path angle of the SLA controller is lower than the conventional controller. On the other hand it will also be shown in Section 4.3 that the maximum achievable pitch attitude of the SLA control law is higher than the 'conventional' control law. Furthermore, airspeed is reduced more with the SLA control law.

Table 1
Actuator limits[23]

Control	Lower actuator limit [deg]	Upper actuator limit [deg]
θ_{1c}	–8.0	8.0
θ_{1s}	–12·5	16·3
θ_0	9·9	25·9
$\theta_{0,tr}$	4·5	36·5

Second, the performance in terms of structural loads and control usage is discussed. The SLA controller keeps the transient pitch link load close to the steady state value (Fig. 9); the conventional controller does not. This proves that the SLA controller adequately suppresses the structural load. This important difference is achieved by a markedly different control strategy. The SLA controller uses more longitudinal cyclic pitch (about 10 degrees more for this particular manoeuvre) and an opposite use of collective pitch. This control strategy difference results in approximately 1 degree more longitudinal flapping (Fig. 10) for the SLA control law. For this particular manoeuvre, the control usage is kept well within the actuator limits. However, there is a significant reduction in the longitudinal cyclic control margin for the SLA control law compared to the conventional controller. It is therefore clear that for more aggressive manoeuvres, the actuator limits will be reached earlier with the SLA controller. So the reduction in structural loads comes at the price of a performance reduction. Furthermore, the opposite use of collective pitch has an implication for the power state. The conventional controller initially demands a larger collective pitch angle and thus the rotor is kept in a so-called power-on state. On the other hand, the SLA controller initially demands a decrease in collective pitch which puts the rotor in a power-off state. The decrease of required engine power in the power-off state reduces the responsiveness of the aircraft (Table 1).

Overall, the results are encouraging and imply that the design method works as desired. It is up to the designer to make a good and balanced trade-off between the different objectives (HQ, SLA), the

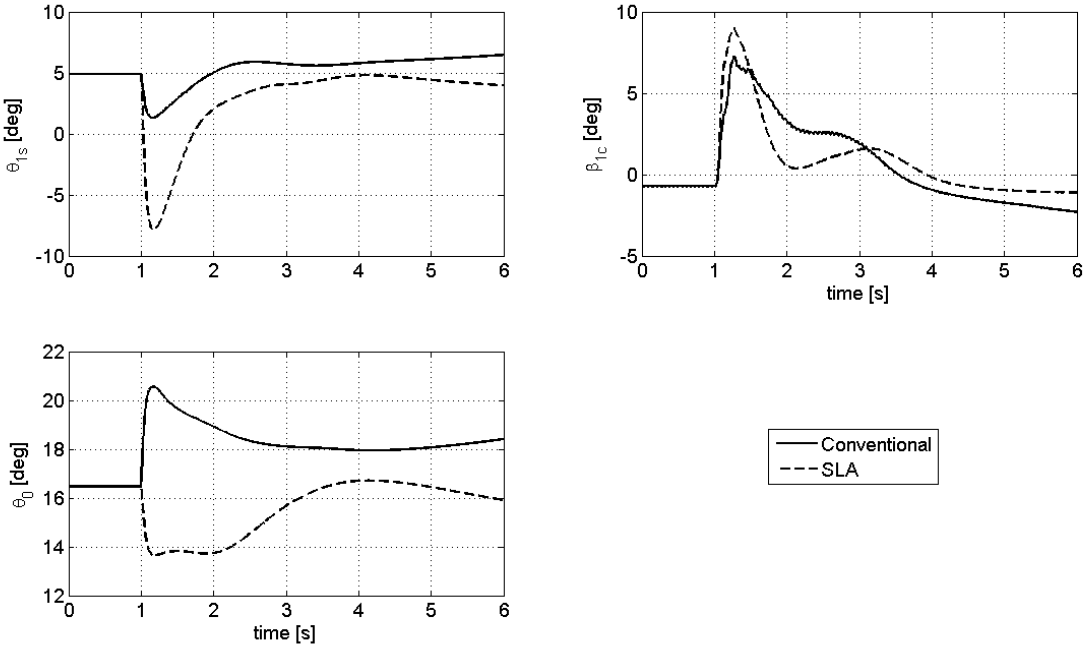


Figure 10. Evaluation of control usage and longitudinal flapping for two control laws on the FGR.

https://doi.org/10.1017/S0001924000002633 Published online by Cambridge University Press

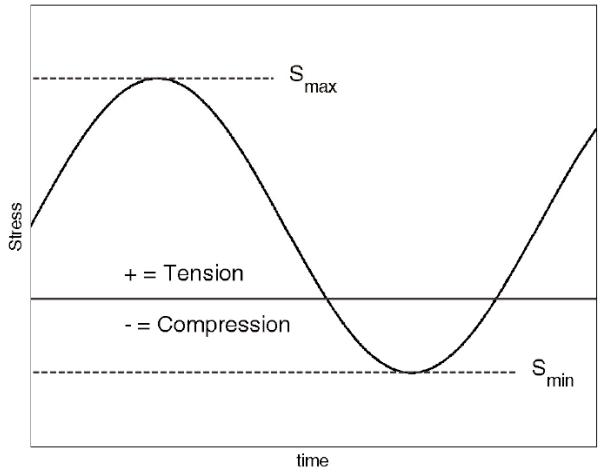


Figure 11. Dynamic loads.

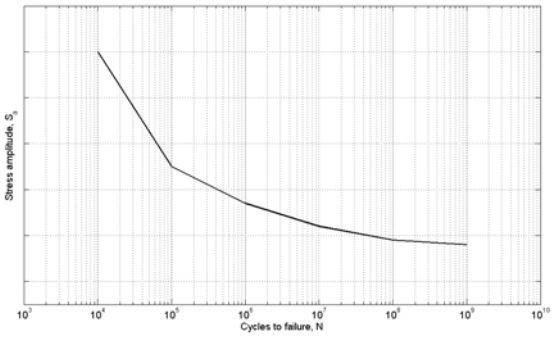


Figure 12. Example *S-N* fatigue curve.

actuator usage and the power state of the rotor. It is not the intention of this paper to present a fully optimised control law. The result also indicates that the use of a 'Coleman' transformation to obtain the pitch link load as a load envelope in the linear domain works effectively. It can in principle be applied to any structural load in the rotating frame.

The analysis of such a novel multi-objective control law with new and already existing structural load metrics is treated in the next section.

4.2 Definition of new structural load metrics

Rotorcraft structural components are subject to both static and dynamic loads. The limit load is defined as the maximum load to be expected in service. The maximum static load that a component has to be able to withstand is defined in the Federal Aviation Regulations (FAR) and the Joint Aviation Requirements (JAR). This is the ultimate load, which is the limit load multiplied by a prescribed factor of safety (usually 1·5). Generally speaking, the structure has to be able to support the ultimate load for at least three-seconds. It is conceivable that a component might fail at a stress level considerably less than the stress level present when the ultimate load is applied. A component can fail due to fatigue whenever it is subjected to dynamic and fluctuating stresses[24].

Rotorcraft components in the rotor system are dynamically loaded. The main frequency at which these components are loaded is the rotor rotational frequency. A dynamic stress can be represented as in Fig. 11.

The sign convention is such that positive stresses are tensile. The maximum stress to be encountered in one cycle is called S_{max}, and the minimum stress is called S_{min}. The oscillatory stress S_a and the mean stress S_m can then be calculated with the following two formulae.

$$S_a = \frac{S_{max} - S_{min}}{2} \quad \ldots (3)$$

$$S_m = \frac{S_{max} + S_{min}}{2} \quad \ldots (4)$$

The approximate number of cycles that will fail a component at a certain mean stress level and at a certain oscillatory load can be determined by laboratory tests. Results from these tests are usually summarised in a so-called *S-N* curve. From this curve one can determine the number of cycles at a certain oscillatory load required to fail the component. The mean stress level has an influence on this curve. A typical *S-N* curve is given in Fig. 12.

An increase in the mean stress will shift the curve up. The curve is generally split into two sections:

- Low cycle fatigue ($< 10^4 - 10^5$ cycles)
- High cycle fatigue ($> 10^5$ cycles)

For some materials, the *S-N* curve has a horizontal asymptote known as the fatigue limit or endurance limit. This limit is the stress below which a fatigue failure does not occur regardless of how many times the load is repeated. Aluminium does not have a fatigue limit that is clearly defined, so it is often taken as the stress at 5×10^8 cycles[25]. The other limit on the *S-N* curve will simply be the stress at which the component fails after one cycle, which is identical to the ultimate load.

Helicopter dynamic components can be designed with different methods with respect to the fatigue life. The most widely used methods are the safe-life method and the damage tolerance method. Other methods in use are e.g. the flaw-tolerance and fault tolerance method[26], which are derivatives of the safe-life and damage tolerance method. The Safe life method works as follows. The oscillatory loads are measured in flight. They are subsequently compared with the appropriate *S-N* curves. The fatigue life can then be calculated with Miner's rule[27], using the flight stresses and the certification spectrum of the aircraft[28]. Miner's rule is a fairly simple but effective rule. If S_a and S_m are known for one cycle, one can calculate the damage D due to one cycle with the *S-N* curve.

$$D_i = \frac{1}{N_i} \quad \ldots (5)$$

N_i is the number of cycles at which the component fails for the oscillatory load S_a and the mean stress S_m. The damage due to one cycle D_i is dimensionless. The total damage D is the sum of the damage done by all the cycles in the certification spectrum. The component will fail when the total damage has accumulated to 1.

$$D = \sum D_i \quad \ldots (6)$$

The component will have to be replaced before the safe life has been reached[28]. A margin of safety (three standard deviations from the mean) is usually applied to the *S-N* curve for this method[26].

https://doi.org/10.1017/S0001924000002633 Published online by Cambridge University Press

The damage tolerance approach on the other hand assumes that there is already a crack present in the component. The time that it takes for this assumed crack to grow to a length where the component will fail is calculated with crack growth data of the component and with the loads that will be encountered in the flight certification spectrum of the aircraft. This time interval is called the crack growth life. Inspections of the component will be conducted frequently enough, based on the crack growth life, to find cracks before they can grow to their critical length[28]. Most rotorcraft components are designed with the safe life method because it is a very simple and effective method.

One of the goals of this study is to define a structural load severity scale, which can be used just like the well-known ADS-33 handling qualities requirements[29]. The following scale is proposed, based on the literature survey described above:

Level 1: Stress level < fatigue limit
Level 2: High cycle fatigue loading
Level 3: Low cycle fatigue loading
Level 4: Stress level > ultimate load

This scale is somewhat similar to the scale (Level A, B, C, D) used by Westland Helicopters[30,31] although the borders between the levels lie at different fatigue loadings. The question remains now, how to transfer this scale to a metric for offline analysis and to a tool for evaluating MTEs. One possible approach for evaluating MTE damage might be the following; the damage done to a component during the MTE can be calculated with Miner's rule. The damage for the borders between the levels for any MTE can also be calculated with Miner's rule:

$$D_{23} = \frac{1}{N_{23}} \frac{\Omega}{2\pi} t_{MTE} \quad \ldots (7)$$

Where D_{23} is the total damage to the component when the manoeuvre is executed with an oscillatory load occurring once every rotor revolution at a stress level on the border of Level 2 and Level 3. The total number of stress cycles is equal to $\frac{\Omega}{2\pi} t_{MTE}$ in which t_{MTE} is the time required for an MTE when it is performed exactly according to the definition in ADS-33. N_{23} is the number of cycles at which the component fails at the stress level on the border of Level 2 and 3. Similar formulas can be derived for the other two borders.

Mission Task Elements:

- Level 1: $D_{MTE} \leq D_{12}$
- Level 2: $D_{12} < D_{MTE} \leq D_{23}$
- Level 3: $D_{23} < D_{MTE} \leq D_{34}$
- Level 4: $D_{34} < D_{MTE}$

Unfortunately *S-N* curves are not always available. Also, one might want to use these scales while still in the design phase of the helicopter when exact dimensions of components are not yet determined or materials are not yet selected. Or one may want to use a load severity scale for more general structural loads such as hub loads. In these cases it is not possible to use the severity scales defined above. The so-called load amplification factor (LAF) is therefore proposed. The LAF is simply the factor with which the steady state oscillatory load ($S_{a,ss}$) at the beginning of a manoeuvre is multiplied during the manoeuvre.

$$LAF = \frac{S_{a,max}}{S_{a,ss}} \quad \ldots (8)$$

At the present moment, no *S-N* curves are available for the pitch link of the FGR. Pavel and Padfield[32] have proposed a structural load metric in combination with a handling quality metric that can be used for high-speed longitudinal manoeuvres with rotorcraft. They are called the agility quickness and the vibratory load quickness.

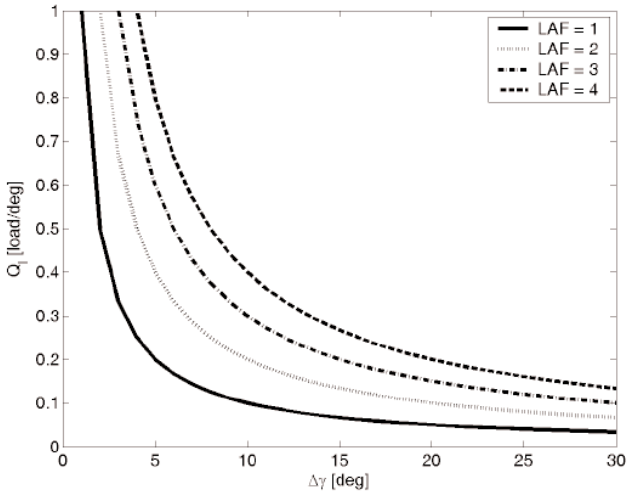


Figure 13. Load amplification factor contours.

$$Q_\gamma \triangleq \frac{n_{z,qs}^{pk}}{\Delta\gamma} \approx \frac{\dot{\gamma}}{\Delta\gamma} \quad \ldots (9)$$

$$Q_l \triangleq \frac{n_{z,pk}^{vib}}{\Delta\gamma} \quad \ldots (10)$$

At high speed, it could be beneficial for a pilot to have control over the flight path angle instead of pitch attitude/rate for most tasks. This is why the well-known pitch attitude quickness has been replaced by flight path angle quickness (Equation 7). The focus in this paper will be on the load quickness parameter because we are primarily interested in whether the structural loads can be reduced. The variable in the load quickness definition represents the peak amplitude in 'g units' in the vibratory components of the hub forces. These forces are divided by the aircraft weight in order to express them as accelerations. This load quickness parameter was used to evaluate the vibratory loads of the FGR for pull-up manoeuvres. It is proposed here to slightly alter the definition of the load quickness parameter to make it applicable to the pitch link load alleviation problem. Hence two definitions are proposed.

$$Q_{l,\gamma} = \frac{F_{pk}}{F_{ss} \cdot \Delta\gamma}, \quad Q_{l,\theta} = \frac{F_{pk}}{F_{ss} \cdot \Delta\theta} \quad \ldots (11)$$

One can be used in combination with the attitude quickness and one with agility quickness. F_{pk} in these formulas is the peak oscillatory pitch link load during a manoeuvre. F_{ss} is the steady state pitch link load at the flight condition under evaluation. Note that the load quickness has the dimension 1/deg which allows the comparison of structural loads amplification experienced during manoeuvres for different rotorcraft types. After evaluation of the two load quickness definitions, conclusions can be drawn upon the advantages and shortcomings of these parameters.

In order to be able to use the load quickness as a design parameter, different structural load levels should be devised. The load amplification factor (LAF) as explained before can be used for this. Constant load amplification factor lines can be calculated by combining Equations 7 and 10.

$$Q_{l,\gamma} = \frac{LAF}{\Delta\gamma} \quad \ldots (12)$$

Four load amplification factor contours are shown in Fig. 13.

https://doi.org/10.1017/S0001924000002633 Published online by Cambridge University Press

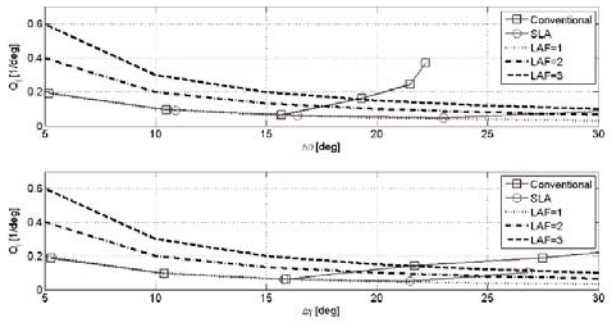


Figure 14. Load quickness plots as a function of pitch attitude change and flight path angle change.

These lines have a similar shape to the well-known ADS-33 handling qualities levels for attitude quickness. The load quickness parameter in combination with the LAF will be used in the next paragraph to evaluate the controller.

4.3 Analysis of the multi-objective longitudinal flight control law

A series of longitudinal step inputs with varying magnitudes was given for both control laws in order to determine the load quickness. Results are presented in Fig. 14 including the constant load amplification factor lines.

The pitch link loads are greatly reduced by the control law that has the SLA functionality built in. The load amplification factor contours allow the amplification of the pitch link load during the pull-up manoeuvre to be determined. For moderate to large amplitude manoeuvres, structural loads are amplified more than 4 times with respect to the steady state value with the conventional control law. The SLA control law only allows an amplification of about 2·5. Conclusions with respect to handling qualities can also be drawn from Fig. 14. With the SLA control law, the achievable flight path angle is limited to approximately 27 degrees. On the other hand, the maximum achievable pitch attitude is only 23 degrees for the conventional control law. Thus the SLA control law can achieve larger pitch attitudes and the conventional control law can achieve larger flight path angles. In terms of handling qualities, it depends on the mission task element whether the conventional control law performs better than the SLA control law. Generally speaking, the achievable flight path angle is more important than the achievable pitch attitude. In terms of structural loads, the SLA control law shows a marked improvement over the conventional control law.

5.0 CONCLUSIONS AND RECOMMENDATIONS

A novel design method has been presented in this paper that enables the flight control system engineer to include SLA objectives into the design of a helicopter longitudinal axis flight control system. The proposed design method is based on *H*-infinity optimisation. This method tries to obtain a stabilising controller that minimises the energy gain of the transfer function from a vector of reference signals to a vector of error signals. The general concept is that the vector of error signals can include structural load objectives as well as traditional handling qualities objectives such as a pitch attitude tracking error.

The method has been applied to a case study centred on the reduction of pitch link loads during high-speed pull up manoeuvres. It is known from the literature that the pitch link loads for this aircraft increase in steady state flight with airspeed and they are magnified significantly during high-speed pull-ups. A novel longitudinal flight control law was therefore design with the new design method, providing a pitch ACAH response type. The objective to minimise the transient pitch link loads was included in the design. The resulting controller was implemented on the nonlinear FGR simulation model and a series of desktop simulations was performed. The pitch link load is effectively reduced by this controller compared to a controller designed along the same lines that did not have the structural load objective.

One must bear in mind that the results obtained in this paper are subject to uncertainties in the FGR model. This is one of the reasons why the *H*-infinity control method is used for the control law design. If the design method is applied to a real-life problem with an actual helicopter, then a thorough examination should be made of the sensitivity of the results to the uncertainties in the helicopter model. Furthermore, the model used for control law design should be validated against flight test data.

The so-called load amplification factor is defined to be used in combination with the load quickness parameter for analysis of the pitch link load. This factor appeared to be very useful for analysis and makes the load quickness non-dimensional. Additionally a structural load severity scale is presented that can be used for analysis of mission task elements with a pilot in the loop. This scale is analogous to the Cooper-Harper handling qualities rating scale. A 'Coleman' transformation of the pitch link loads had to be made in the design phase, in order to include the load in the linear model that was used for control law design. This transformation was effective to represent the load acting in the rotating frame as a load envelope in the linear model.

It is recommended for future work that a flight control system for the complete flight envelope of the FGR is developed, including a structural load objective. The load quickness parameter, load amplification factors and the traditional ADS-33 handling qualities requirements should subsequently be used for offline analysis. The structural load severity scale can then be tested with a pilot in the loop.

ACKNOWLEDGEMENTS

The research presented in this paper is funded by the UK Engineering and Physical Sciences Research Council through Research Grant GR/S42354/01.

REFERENCES

1. PROUTY, R.W. *Helicopter Aerodynamics – Ray Prouty's Rotor and Wing Columns 1979-1992*, 2004, Helobooks a division of Mojave books LLC, Mojave, CA, USA.
2. LOY, K. Carefree handling and its applications to military helicopters and missions, May 1997, American Helicopter Society's 53rd annual forum, Virginia Beach, VA, USA.
3. MANIMALA, B.J., WALKER, D.J., PADFIELD, G.D., VOSKUIJL, M. and GUBBELS, A.W. Rotorcraft simulation modelling and validation for control law design, *Aeronaut J*, February 2007, **111**, (1116), pp 77-88.
4. WALKER, D.J., VOSKUIJL, M., MANIMALA, B.J. and GUBBELS, A.W. Nonlinear attitude control laws for the Bell 412 helicopter, *AIAA J Guidance, Control and Dynamics*, February-March 2008, **31**, (1), pp 44-52.
5. PADFIELD, G.D. and WHITE, M.D. Flight simulation in academia – HELIFLIGHT in its first year of operation at the University of Liverpool, *Aeronaut J*, September 2003, **107**, (1075), pp 529-538.
6. GUBBELS, A.W. and CARIGNAN, S.J.R.P. The NRC Bell 412 Advanced Systems Research Aircraft — a new facility for airborne simulation, *Canadian Aeronautics and Space J*, June 2000, **46**, (2), pp 106-115.
7. BAILLIE, S.W., KERELIUK, S., MURRAY MORGAN, J. and HUI, K. An evaluation of the dynamics and handling quality characteristics of the Bell 412HP helicopter, *Canadian Aeronautics and Space J*, March 1994, **40**, (1), pp 32-46.
8. CURTISS, H. C., CARSON, F., HILL, J., QUACKENBUSH, T., Technical note – Performance of a Sikorsky S-61 with a new main rotor, *J American Helicopter Soc*, July 2003.

https://doi.org/10.1017/S0001924000002633 Published online by Cambridge University Press

9. KUFELD, R.M. and BOUSMAN, W.G. High load conditions measured on a UH-60A in maneuvering flight, *J American Helicopter Soc*, July 1998, **43**, (3), pp 202-211.
10. CRESAP, W.L., MYERS, A.W. and VISWANATHAN, S.P. Design and development tests of a four-bladed light helicopter rotor system, May 1978, 34th annual forum of the American Helicopter Society.
11. CRESAP, W.L. and MYERS, A.W. Design and development of the model 412 helicopter, 36th annual forum of the American Helicopter Society, May 1980, Washington, DC, USA.
12. YEN, J.G. and WELLER, W.H. Analysis and application of compliant rotor technology September 1980, Sixth European Rotorcraft and Powered Lift Aircraft Forum, Bristol, UK.
13. BAILEY, F.J. A simplified theoretical method of determining the characteristics of a lifting rotor in forward flight, 1941, NACA report 716.
14. MANSUR, M.H. and TISCHLER, M.B. An empirical correction for improving off-axis response in flight mechanics helicopter models, *J American Helicopter Soc*, 1998, **43**, (2), pp 94-102.
15. KUFELD, R.M. and BOUSMAN, W.G. UH-60A helicopter rotor airloads measured in flight, *Aeronaut J*, May 1997, **101**, (1005), pp 217-227.
16. CURTISS, H.C. and CARSON, F. Further improvements to the S-61 helicopter, September 2005, 31st European Rotorcraft Forum, Florence, Italy.
17. WALKER, D.J., MANIMALA, B.J., VOSKUIJL, M. and GUBBELS, A.W. Multivariable control of the Bell 412 helicopter, 2006, Proceedings of the IEEE Conference on Decision and Control, No 4177255, pp 1527-1535.
18. KWAKERNAAK, H. Robust control and *H*-infinity optimization – tutorial paper, *Automatica*, 1993, **29**, (2), pp 255-273.
19. MANIMALA, B., PADFIELD, G.D., WALKER, D., NADDEI, M., VERDE, L., CINIGLIO, U., ROLLET, P. and SANDRI, F. Load alleviation in tilt rotor aircraft through active control: modelling and control concepts, *Aeronaut J*, April 2004, **108**, (1082), pp 169-184.
20. PADFIELD, G.D. *Helicopter Flight Dynamics*, 1996, Blackwell Science, Oxford, UK.
21. COLEMAN, R.P. and FEINGOLD, A.M. Theory of self-excited mechanical oscillations of helicopter rotors with hinged blades, 1951, NACA 1351.
22. GAHINET, P., NEMIROVSKI, A., LAUB, A.J., and CHILALI, M. LMI Control Toolbox, for use with MATLAB®, 1995, The Math Works, Natick, MA, USA.
23. HOWLETT, J.J. UH60A Black Hawk engineering simulation program: Volume I — Mathematical model, December 1981, NASA CR 166309.
24. CALLISTER, W.D. *Materials Science and Engineering an Introduction*, 1997, John Wiley & Sons.
25. GERE, J.M. and TIMOSHENKO, S.P. *Mechanics of Materials*, 1987, Chapman & Hall, London, UK.
26. FORTH, S.C., EVERETT, R.A., NEWMAN, J.A., A novel approach to rotorcraft damage tolerance, September 2002, Sixth Joint FAA/DoD/NASA aging aircraft conference, USA.
27. MINER, M.A. Cumulative damage in fatigue, *ASME J Applied Mechanics*, 1945, **12**, pp PA159-164.
28. MICHEAL, J., COLLINGWOOD, G., AUGUSTINE, M. and CRONKHITE, J. Continued evaluation and spectrum development of a health and usage monitoring system, May 2004, DOT/FAA/AR-04/6, Fort Worth, TX, USA.
29. ANONYMOUS. ADS-33E PRF, Aeronautical design standard performance specification, handling qualities requirements for military rotorcraft.
30. MARTYN, A.W., CHARLTON, M.T. and PADFIELD, G.D. Vehicle structural fatigue issues in rotorcraft flying qualities testing, September 1995, 21st European Rotorcraft Forum, St Petersburg, Russia.
31. ANONYMOUS. Monitor limits for MoD flight trials, 3 February 1994, WHL, SDR 84, **3**.
32. PAVEL, M.D. and PADFIELD, G.D. Defining consistent ADS-33 metrics for agility enhancement and structural loads alleviation, June 2002, 58th Annual Forum of the American Helicopter Society, Montreal, Canada.

https://doi.org/10.1017/S0001924000002633 Published online by Cambridge University Press